

Weak Pinning and Hexatic Order in a Doped Two-Dimensional Charge-Density-Wave System

Hongjie Dai, Huifen Chen, and Charles M. Lieber

Departments of Chemistry and Applied Physics, Columbia University, New York, New York 10027

(Received 11 July 1990; revised manuscript received 25 February 1991)

Scanning-tunneling microscopy has been used to characterize the effects of Nb impurities on the incommensurate charge-density-wave (CDW) phase in $1T\text{-TaS}_2$. Real- and reciprocal-space data indicate that disorder in the CDW is due to dislocations and small random rotations of the CDW. The dislocations destroy translational order; however, calculations show that the orientational order is long range. These results are consistent with weak pinning and suggest the possibility of a hexatic CDW phase. The similarity of our data to results obtained for other two-dimensional systems is discussed.

PACS numbers: 71.45.Lr, 61.16.Di, 64.70.Kb

Determining the nature of the interaction between impurities and a charge-density wave (CDW) is essential to understanding the static and dynamic properties of the CDW state.¹⁻⁶ In general, two regimes, strong and weak pinning, have been defined to describe the strength of the interaction of impurities with a CDW. In strong pinning the impurity potential dominates the elastic energy of the CDW and pins the CDW phase at each impurity site.³ In weak pinning, the CDW breaks up into constant-phase regions pinned to the random impurity distribution; that is, the pinning is collective.³ There has been considerable theoretical and experimental controversy regarding weak pinning in CDW systems,³⁻⁹ in large part because data characterizing the structural evolution of the CDW order with doping have been ambiguous. More generally, weak or collective pinning is also believed to play an important role in other physical systems, most notably the flux-line lattice of the high-temperature copper-oxide superconductors.¹⁰ For these materials it has been suggested that weak pinning gives rise to a hexatic vortex-glass state in which the flux-line lattice exhibits long-range orientational order but only short-range translational order.^{10,11}

Much of the experimental work that has addressed the nature of impurity pinning in CDW systems has focused on transport measurements.^{1,2} Unfortunately, the interpretation of these data in terms of strong or weak pinning has often been controversial.³⁻⁹ An unambiguous resolution of the nature of pinning requires that the structure of the CDW phase be determined in the presence of dopants.⁷ Scanning-tunneling microscopy (STM) can determine the structure of a CDW in real space,^{12,13} and hence should provide a direct method to address the nature of pinning. In previous STM studies we investigated the effect of nonisoelectronic impurities on the CDW phase.¹⁴ This work illustrates that STM can be used as a direct structural probe of doped CDW materials; however, the interpretation of these earlier results is complicated since impurity pinning was not studied in the incommensurate state, i.e., the CDW was already pinned to the lattice in the absence of impurities.

In this Letter we present new experimental data and a new quantitative analysis for the incommensurate CDW

phase in Nb-doped $1T\text{-TaS}_2$, $\text{Nb}_x\text{Ta}_{1-x}\text{S}_2$, that provide strong structural evidence for the weak-pinning model. Real- and reciprocal-space analyses of the images indicate that Nb impurities cause dislocations and small rotations of the CDW. The dislocations destroy translational order of the CDW, although the orientational order appears to be long range. Calculations of the orientational correlation function indicate that the orientational order decays much more slowly than translational order at low impurity concentrations. Long-range orientational order and short-range translational order are consistent with weak (i.e., collective) pinning and suggest that the CDW phase is possibly a hexatic glass. These data are strikingly similar to results obtained for two-dimensional binary random arrays¹⁵ and the flux-line lattice in superconductors.^{10,11}

Single crystals of $\text{Nb}_x\text{Ta}_{1-x}\text{S}_2$ ($x=0, 0.04, 0.07, 0.10$) were grown by iodine-vapor transport in a 70°C gradient. Bulk and surface analyses were used to verify the concentration of Nb and the stoichiometry of the crystals. The incommensurate to nearly commensurate CDW transition temperatures for the $x=0, 0.04, 0.07,$ and 0.10 samples were determined from resistivity measurements and found to agree with previous reports.^{2,16} STM images were recorded in the incommensurate state on crystals with characterized transition temperatures using a commercial instrument (Nanoscope, Digital Instruments, Inc.) that has been modified for variable-temperature operation. The temperature was monitored with a calibrated thermocouple placed directly behind the sample. Other experimental details have been described previously.¹⁴

The essential experimental results from our studies are shown in Fig. 1. The STM images of the $x=0, 0.04, 0.07,$ and 0.10 $\text{Nb}_x\text{Ta}_{1-x}\text{S}_2$ single crystals were recorded at 380, 340, 315, and 298 K, respectively, to ensure that the samples were in the incommensurate state since the CDW is already pinned to the lattice in the low-temperature commensurate and nearly commensurate states.¹⁷ Temperature variations within the incommensurate state did not affect the structure shown in the images. There are several features evident from analysis of the images. First, we find that the Nb impurities induce

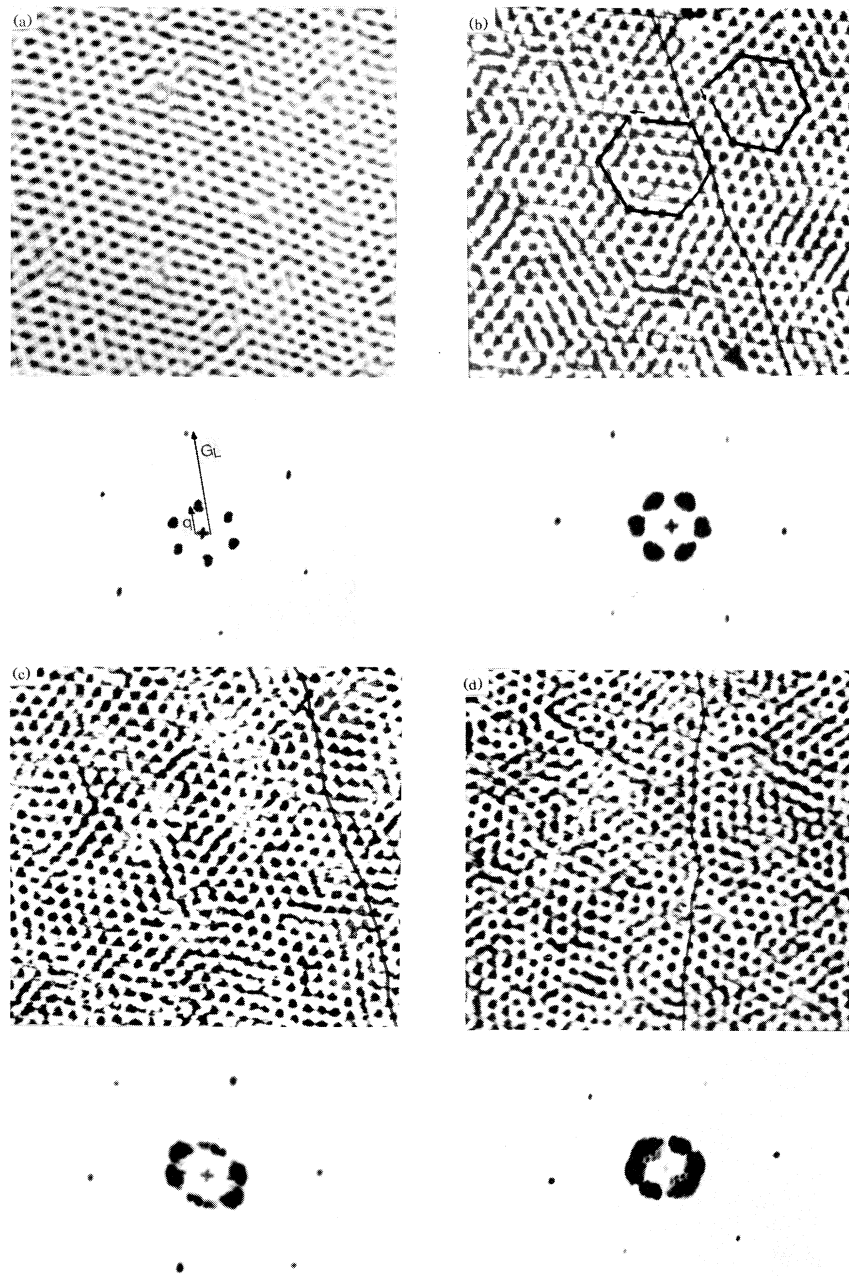


FIG. 1. $30 \times 30\text{-nm}^2$ gray-scale images of (a) $1T\text{-TaS}_2$, (b) $\text{Nb}_{0.04}\text{Ta}_{0.96}\text{S}_2$, (c) $\text{Nb}_{0.07}\text{Ta}_{0.93}\text{S}_2$, and (d) $\text{Nb}_{0.1}\text{Ta}_{0.9}\text{S}_2$ recorded with a tunneling current of 2 nA and a bias voltage of 11 mV. The images are displayed with an inverted gray scale; i.e., the black spots correspond to CDW maxima. Two dislocation loops are highlighted in (b). 2DFT power spectra of images corresponding to these samples are shown below the images. The atomic lattice (G_L) and CDW (q) wave vectors are indicated below (a).

dislocations in the CDW lattice. Dislocation pairs in which the coordination of the CDW maxima is 5 or 7 (versus 6 for a perfect lattice) and other defects are apparent in the images; trapped defects are explicitly highlighted by the two dislocation loops in Fig. 1(b). The density of dislocations, which are observed in every image of Nb-doped samples, increases with increasing

niobium concentration ($x=0.04\text{--}0.10$). The distance between dislocations is, however, greater than the average impurity spacing and thus it is unlikely that these defects are due to strong pinning. Additionally, while it is known that dislocations destroy translational order, orientational order can remain long range in the presence of these defects.^{11,15,18,19}

We have qualitatively assessed the orientational order by drawing lines along a principle CDW direction in the images. These lines illustrate that the average orientation of CDW is approximately constant (i.e., the order is long range), although there are small rotations of the CDW orientation with respect to this average direction in the Nb-doped samples. These small rotations are readily observed by viewing the images at a glancing angle along the indicated lines. Analyses of atomic-resolution images demonstrate that the rotations are not due to instrumental artifacts since the underlying atomic lattice is undistorted.

To further illustrate these points we have calculated the two-dimensional Fourier transform (2DFT) of images of the $x=0-0.10$ samples; these results are shown below the real-space images in Fig. 1. As a reference for our experiment the 2DFT of pure TaS_2 shows sharp first-order peaks corresponding to the hexagonal atomic lattice and CDW superlattice as expected. In contrast, the 2DFTs of the $x=0.04, 0.07,$ and 0.10 images show distinct radial broadening and angular elongation of the CDW peaks, although the atomic lattice spots are sharp in all cases. The radial broadening of the CDW peaks for the Nb-doped samples indicates a lack of translational order. We estimate¹⁵ from the average radial widths determined from several $x=0.04, 0.07,$ and 0.10 2DFTs that the translational correlation lengths are about 4, 3, and 2 CDW wavelengths, respectively. These results are clearly consistent with the proposal that the dislocations detected in our images destroy translational order.

The angular elongation of the CDW peaks in the 2DFT, up to $\pm 15^\circ$ in the $\text{Nb}_{0.1}\text{Ta}_{0.9}\text{S}_2$ sample, is consistent with rotations of the CDW determined directly from the real-space images. The increase in elongation with increasing concentration of Nb also indicates a decrease in orientational order. Recently, there has been some controversy regarding the CDW-lattice orientation in the nearly commensurate state of 17-TaS_2 determined from real-space²⁰ versus reciprocal-space²¹ STM data. This disagreement has centered on a small difference in orientation, $\approx 1^\circ$, obtained from the real-space versus 2DFT analyses. Herein, we note that both analysis methods yield the same picture (i.e., dislocations that destroy translational order and significant rotations of the CDW), and thus we believe that these results reflect the intrinsic effect of Nb impurity pinning and are not due to an artifact of our analysis.

Previous studies have shown that while weak or collective pinning leads to short-range translational order, the orientational order will be long range.^{10,22} Our estimates of the translational correlation length are clearly consistent with short-range order, and, furthermore, the STM images and 2DFT indicate that orientational order may be long range at small values of x . The real-space images also bear a striking resemblance to other two-dimensional systems such as the flux-line lattice in the high- T_c superconductor Bi-Sr-Ca-Cu-O,¹¹ and binary

random arrays of hard spheres.¹⁵ The phase of these latter systems has been assigned to the hexatic state which exhibits long-range orientational order and short-range translational order.

To estimate the orientational order quantitatively and explore this similarity further we have calculated the orientational correlation function $G_6(r)$.^{11,15,18,19} These calculations were carried out for the bond-orientational order parameter $\psi_6(r) = \sum \exp(i6\theta_j)$, where θ_j is the angle with respect to the x axis of the bond between the CDW maximum located at r and its j th nearest neighbor.^{15,19} The plots of $G_6(r)$ for the $x=0-0.1$ samples are shown in Fig. 2 and represent a key finding of this study. At present we have not yet carried out extensive statistical averaging of our results, and thus we cannot be certain about detailed fits to $G_6(r)$. The trends shown in Fig. 2 are, however, significant and reproducible. As a reference, $G_6(r)$ for the CDW lattice in pure TaS_2 shows little decay, as expected for a crystalline phase. The $G_6(r)$ determined for several $x=0.04$ images decay slowly with r and can be fitted by a power law $r^{-\eta}$ with $\eta=0.18 \pm 0.03$.²³ For the $x=0.07$ and 0.10 materials $G_6(r)$ oscillates due to insufficient averaging and cannot be fitted with either a power law or exponential decay. The orientational order obviously decreases, however, from $x=0.04$ to 0.10 .

Previous work has shown that the long-range orientational order of a hexatic phase should yield a power-law decay for $G_6(r)$, while $G_6(r)$ will decay exponentially for less ordered amorphous or liquidlike phases.^{15,18,19} We can fit our data for the $x=0.04$ images by a power-law decay, although at present the calculations have not been carried out to sufficiently large r to rule out an exponential decay. However, irrespective of the fit the orientational order decays much more slowly than the translational order, as expected for a hexatic.¹⁵ These results

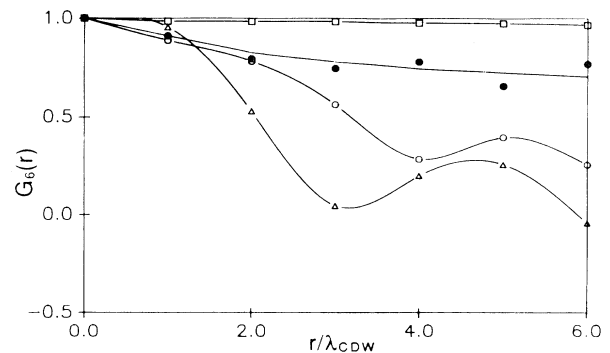


FIG. 2. The orientational correlation function $G_6(r)$ calculated from images of TaS_2 (\square), $\text{Nb}_{0.04}\text{Ta}_{0.96}\text{S}_2$ (\bullet), $\text{Nb}_{0.07}\text{Ta}_{0.93}\text{S}_2$ (\circ), and $\text{Nb}_{0.1}\text{Ta}_{0.9}\text{S}_2$ (\triangle) materials, where λ_{CDW} is the CDW period. The lines through the TaS_2 , $\text{Nb}_{0.07}\text{Ta}_{0.93}\text{S}_2$, and $\text{Nb}_{0.1}\text{Ta}_{0.9}\text{S}_2$ data are shown only as a guide; the curve through the $\text{Nb}_{0.04}\text{Ta}_{0.96}\text{S}_2$ data corresponds, however, to a power-law fit ($r^{-\eta}$) with $\eta=0.15$ for $r/\lambda \geq 1$.

are similar to the quenched-in disorder observed for binary random arrays of spheres,¹⁵ and the flux-line lattice observed in magnetic decoration experiments on Bi-Sr-Ca-Cu-O.¹¹ Notably, in the case of the flux-line lattice theoretical analyses have shown that the long-range orientational order and short-range translational order characteristic of a hexatic state arise from collective or weak pinning.¹⁰ Consideration of these results and our data thus strongly suggests that the pinning of the incommensurate CDW in TaS₂ by Nb impurities is weak. It is also interesting to speculate whether the disorder in the CDW represents snapshots of "melting" as a function of x , where at $x=0$ the phase is crystalline, at $x \approx 0.04$ it is hexatic, and for $x \geq 0.07$ it is amorphous. Although additional studies will be necessary to demonstrate this proposal, our results show that these Nb-doped materials represent a new experimental system in which to explore systematically the consequences of disorder.

In conclusion, we believe that these studies of impurity pinning of the incommensurate CDW in Nb-doped TaS₂ are significant in several respects. First, the observation of dislocations, long-range orientational order, and short-range translational order in STM images of the Nb-doped materials strongly suggests that pinning of the incommensurate CDW is weak or collective. Second, we believe that calculations of the orientational (and translational) correlation functions, applied here for the first time to STM results, represent an important method for quantifying disorder in STM experiments. Lastly, our results suggest that the impurity-induced disorder in this CDW system is analogous to that observed in other two-dimensional systems, and thus we believe that further studies of these well-defined Nb _{x} Ta _{$1-x$} S₂ materials should lead to an improved understanding of quenched disorder and melting in two-dimensional systems.

C.M.L. acknowledges support of this work by the Air Force Office of Scientific Research, and the David and Lucile Packard and National Science Foundations.

¹G. Gruner, Rev. Mod. Phys. **60**, 1129 (1988); G. Gruner and A. Zettl, Phys. Rep. **119**, 117 (1985).

²J. A. Wilson, F. J. DiSalvo, and S. Mahajan, Adv. Phys. **24**, 117 (1975).

³H. Fukuyama and P. A. Lee, Phys. Rev. B **17**, 535 (1978); P. A. Lee and T. M. Rice, *ibid.* **19**, 3970 (1979).

⁴S. N. Coppersmith, Phys. Rev. Lett. **65**, 1044 (1990).

⁵J. R. Tucker, Phys. Rev. B **40**, 5447 (1989).

⁶J. Bardeen, Phys. Rev. Lett. **64**, 2297 (1990).

⁷E. Sweetland, C-Y. Tsai, B. A. Wintner, J. D. Brock, and R. E. Thorne, Phys. Rev. Lett. **65**, 3165 (1990).

⁸J. R. Tucker, Phys. Rev. Lett. **65**, 270 (1990); J. C. Gill, Phys. Rev. Lett. **65**, 271 (1990).

⁹R. E. Thorne and J. McCarten, Phys. Rev. Lett. **65**, 273 (1990).

¹⁰E. M. Chudnovsky, Phys. Rev. Lett. **65**, 3060 (1990); Phys. Rev. B **40**, 11355 (1989).

¹¹C. A. Murray, P. L. Gammel, D.J. Bishop, D. B. Mitzi, and A. Kapitulnik, Phys. Rev. Lett. **64**, 2312 (1990).

¹²R. V. Coleman, B. Giambattista, P.K. Hansma, A. Johnson, W. W. McNairy, and C. G. Slough, Adv. Phys. **37**, 559 (1988).

¹³G. Gammie, J. S. Hubacek, S. L. Skala, R. T. Brockenbrough, J. R. Tucker, and J. W. Lyding, Phys. Rev. B **40**, 9529 (1989); C. G. Slough and R. V. Coleman, *ibid.* **40**, 8042 (1989).

¹⁴X. L. Wu and C. M. Lieber, Phys. Rev. B **41**, 1239 (1990); X. L. Wu, P. Zhou, and C. M. Lieber, Phys. Rev. Lett. **61**, 2604 (1988); H. Chen, X. L. Wu, and C. M. Lieber, J. Am. Chem. Soc. **112**, 3326 (1990).

¹⁵D. R. Nelson, M. Rubinstein, and F. Spaepen, Philos. Mag. A **46**, 105 (1982).

¹⁶F. J. DiSalvo, J. A. Wilson, B. G. Bagley, and J. V. Waszczak, Phys. Rev. B **12**, 2220 (1975).

¹⁷W. L. McMillan, Phys. Rev. B **12**, 1187 (1975).

¹⁸D. R. Nelson and B. I. Halperin, Phys. Rev. B **19**, 2457 (1979).

¹⁹C. A. Murray, W. O. Sprenger, and R. A. Wenk, Phys. Rev. B **42**, 688 (1990).

²⁰X. L. Wu and C. M. Lieber, Phys. Rev. Lett. **64**, 1150 (1990); Science **243**, 1703 (1989).

²¹C. G. Slough, W. W. McNairy, R. V. Coleman, J. Garnaes, C. B. Prater, and P. K. Hansma, Phys. Rev. B **42**, 9255 (1990).

²²A. I. Larkin and Y. N. Ovchinnikov, J. Low Temp. Phys. **34**, 409 (1979).

²³The preliminary calculations for the $x=0.04$ samples can be fitted with either an algebraic or an exponential decay since they have not been carried out to large r . The decay of $G_6(r)$ is, however, significantly longer range than observed for the translational correlation function irrespective of the fitting function, and hence we believe that the trends discussed herein are significant. Detailed calculations of the orientational and translational correlation functions are currently in progress and will be discussed in a subsequent publication.

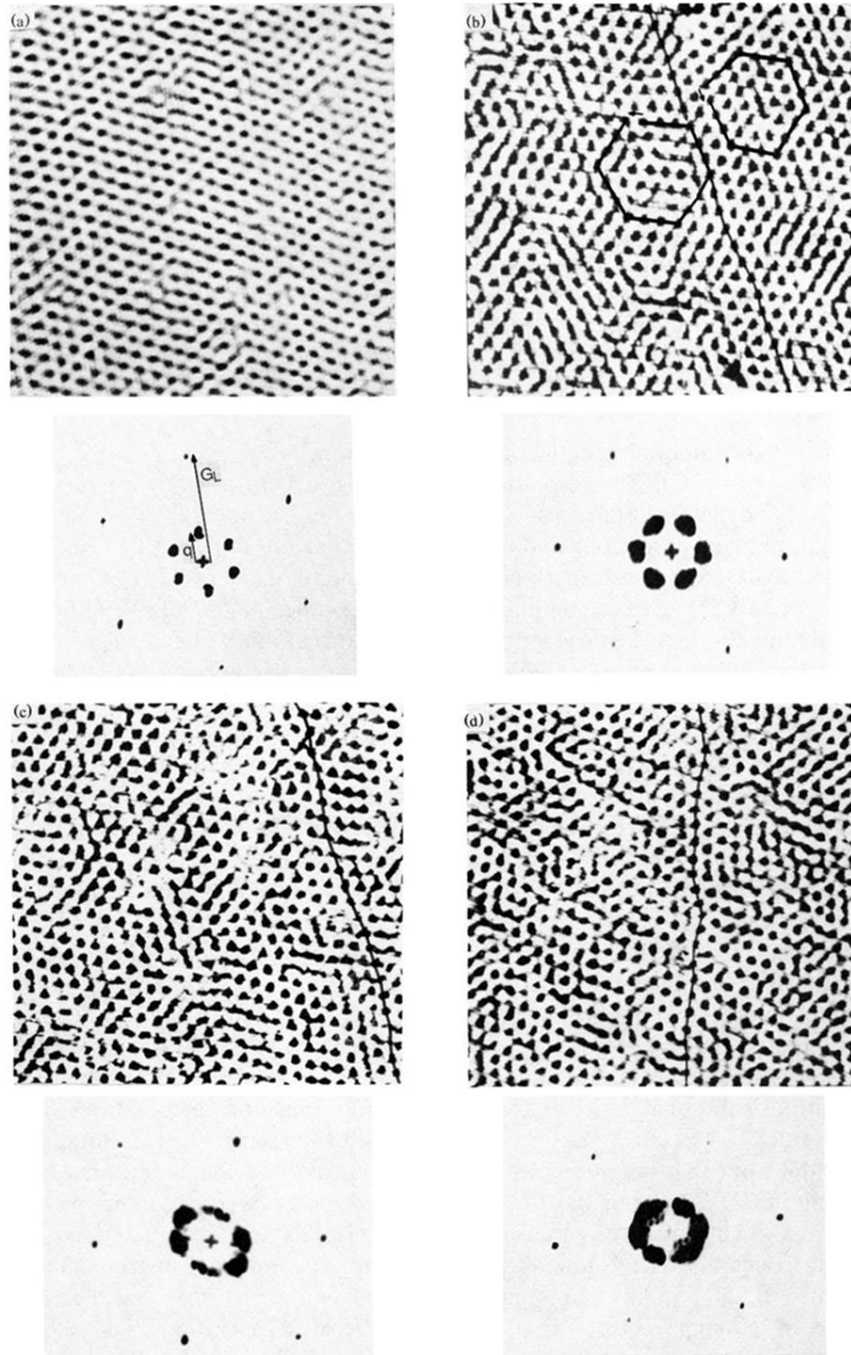


FIG. 1. $30 \times 30\text{-nm}^2$ gray-scale images of (a) $1T\text{-TaS}_2$, (b) $\text{Nb}_{0.04}\text{Ta}_{0.96}\text{S}_2$, (c) $\text{Nb}_{0.07}\text{Ta}_{0.93}\text{S}_2$, and (d) $\text{Nb}_{0.1}\text{Ta}_{0.9}\text{S}_2$ recorded with a tunneling current of 2 nA and a bias voltage of 11 mV. The images are displayed with an inverted gray scale; i.e., the black spots correspond to CDW maxima. Two dislocation loops are highlighted in (b). 2DFT power spectra of images corresponding to these samples are shown below the images. The atomic lattice (G_L) and CDW (q) wave vectors are indicated below (a).